An optimization model for planning testing and control strategies to limit the spread of a pandemic -The case of COVID-19

Adam Abdin, Yi-Ping Fang, Aakil Caunhye, Douglas Alem, Anne Barros, Enrico Zio

An optimization model for planning testing and control strategies to limit the spread of a pandemic - The case of COVID-19

Adam F. Abdin[a,*], Yi-Ping Fang[a,b], Aakil Caunhye[c], Douglas Alem[c], Anne Barros[a,b], Enrico Zio[d,e]

[a] *Laboratoire Genie Industriel, CentraleSupélec, Université Paris-Saclay*
3 Rue Joliot Curie, 91190 Gif-sur-Yvette, France
[b] *Chair on Risk and Resilience of Complex Systems*
[c] *University of Edinburgh Business School, Edinburgh, United Kingdom*
[d] *Mines ParisTech, PSL Research University, CRC, Sophia Antipolis, France*
[e] *Department of Energy, Politecnico di Milano, Italy*

Abstract

The global health crisis caused by the coronavirus SARS-CoV-2 has highlighted the importance of efficient disease detection and control strategies for minimizing the number of infections and deaths in the population and halting the spread of the pandemic. Countries have shown different preparedness levels for promptly implementing disease detection strategies, via mass testing and isolation of identified cases, which led to a largely varying impact of the outbreak on the populations and health-care systems. In this paper, we propose a new pandemic resource allocation model for allocating limited disease detection and control resources, in particular testing capacities, in order to limit the spread of a pandemic. The proposed model is a novel epidemiological compartmental model formulated as a mixed-integer non-linear optimization that is suitable to address the inherent non-linearity of an infectious disease progression within the population. A number of novel features are implemented in the model to take into account important disease characteristics, such as asymptomatic infection and the distinct risk levels of infection within different segments of the population. Moreover, a method is proposed to estimate the vulnerability level of the different communities impacted by the pandemic and to explicitly consider equity within the resource allocation problem. The model is validated against real data for a case study of COVID-19 outbreak in France and our results provide various insights on the optimal testing intervention time and level, and the impact of the optimal allocation of testing resources on the spread of the disease among regions. The results confirm the significance of the proposed modeling framework for informing policymakers on the best preparedness strategies against future disease outbreaks.

Keywords: (S) Decision Support Systems, Pandemic Control, Covid-19, Disaster Preparedness, Mixed-Integer Non-linear Programming

1. Introduction

During the early days of January 2020, it was reported that a number of pneumonia cases, identified by the end of 2019 and, at the time, of an unknown aetiology, were, in fact, caused by a novel coronavirus disease later labeled as SARS-CoV-2. In the months that followed, this novel coronavirus, now popularly

*Corresponding author
Email address: adam.abdin@centralesupelec.fr (Adam F. Abdin)

known as COVID-19, started to rapidly spread across the globe, resulting in an exponential increase in the number of infections and hospitalizations of severe cases. With hospitals in many countries reaching their maximum operational limits and with the rapidly increasing number of deaths caused by the virus, the World Health Organization (WHO) declared the outbreak as a global pandemic. Since the first identified cases in January 2020, the number of confirmed cases and deaths related to COVID-19 have surpassed 80 million and 1.7 million, respectively (WHO et al., 2020).

Early reports compared the progression of the COVID-19 virus among several nations, including China, Italy, France and South Korea, to name a few, showing how the difference in preparedness and control policies implemented, such as mass testing, lock-downs, contact tracing and case isolation seemed to be resulting in major differences in the rates of infected individuals, hospitalizations and deaths among those countries (Hsiang et al., 2020). These differences in early control policies are often the result of a variety of factors, including cultural, social, economic, political, among others (Yan et al., 2020). However, a major contributor to the efficiency in implementing a successful control measure is the degree of preparedness within the system (country/region) to deploy and allocate the proper resources in order to limit the spread of a contagious disease. A notable example is the preparedness level seen in the case of the Republic of Korea. The Republic of Korea was successful in identifying a large number of cases very early on, as a result of implementing a massive testing strategy, reaching around 20,000 tests per day in less than 6 weeks since they identified the first case (Sung et al., 2020). The strategy was successful in significantly slowing down the spread of the disease without enforcing city-wide lock-downs or collapse of the national health-care system. In other cases, pandemic responses have been criticized as resulting in high peaks of infections and deaths during the early phase of the outbreak, particularly, due to the lack of identification of cases via mass testing and contact tracing (Moatti, 2020).

Testing, case-isolation and control strategies have been shown to be effective measures to control the spread of contagious diseases, including the current COVID-19 pandemic (Madubueze et al., 2020; Aleta et al., 2020; Wells et al., 2020). However, with regards to the actual levels of preparedness for rapidly implementing testing strategies and allocating testing capacities among different regions, policymakers face a number of planning challenges. Testing resources may be naturally limited at the onset of the outbreak of a new disease, as testing technologies are still being developed. Other factors, such as, distribution times, test administration times and the number of trained staff available to perform the procedure and interpret the results, may also contribute to limit the capability to effectively allocate massive testing capacities. Furthermore, in the context of the COVID-19 outbreak, the decisions for controlling the pandemic spread should take into account disease specific attributes, among which, the difference in severity of symptoms and risk factors within the population (elders and those with underlying health conditions are more prone to develops severe symptoms compared to younger and healthier individuals (Jordan et al., 2020)), the high rate of transmission of the disease among *asymptomatic* individuals (Moghadas et al., 2020) and the impact of population mobility between regions (Guan et al., 2020), particularly from infected-asymptomatic individuals who are harder to identify. Finally, a major challenge for policymakers for allocating limited control resources among regions is to ensure an equitable distribution of these resources. Despite the fact that there is little consensus about the meaning of equity, it is broadly accepted in public health that an equitable allocation of resources help to mitigate disparities and improve health outcomes (Braveman, 2006). An equitable public preparedness and management strategy does not solely

depend on the character and severity of the disaster in and of itself, but also on the vulnerability of the particular communities impacted by it. Whereas public health disasters such as the COVID-19 pandemic do not, themselves, create the conditions of health access inequities in a population, they accentuate existing ones and make it so that vulnerable communities suffer the most (Alberti et al., 2020).

The aim of this paper is to provide an optimization modeling framework to help policymakers optimally planning and evaluating decisions on allocating scarce disease detection and control resources in order to mitigate the spread of a pandemic. Since a pandemic progression within a population is an inherently non-linear phenomenon, the proposed model is an explicitly formulated non-linear optimization model that captures key disease transmission characteristics and non-linear transition dynamics. In addition, the modeling framework proposed takes into account specific characteristics of the COVID-19 pandemic, most notably, the possibility of asymptomatic exposure and infection, as well as the distinct risk levels of infection for different segments of the population. The spatio-temporal aspect of the decision making is further considered by accounting for population mobility between regions. Finally, the proposed modeling framework is extended to account for equity considerations for the exposed and vulnerable communities within the decision-making problem. The relevance of the modeling framework is validated with a real case study, first by validating the model predictions against real pandemic control measures and the resulting disease transmission dynamics, and subsequently, by showing the significance of the results for a range of intervention policies. To the best of our knowledge, this study is the first attempt to formulate and address the problem of allocating testing and control resources as a Mixed-Integer Non-Linear (MINLP) optimization model for controlling an infectious disease outbreak.

2. Literature review and paper contributions

There is a large body of literature that deals with modeling infectious diseases within a decision making framework (Dasaklis et al., 2012). One of the most prominent modeling approaches that have proven its usefulness for modeling epidemics is the SIR compartmental model proposed by (Kermack and McKendrick, 1927) and its various extensions (see for example (van den Driessche, 2008)). The basic SIR model separates the population in three groups: susceptible individuals (S) who can get the disease, those infected (I), and those removed from the population (R) due to recovery, death or immunity. In the majority of studies, these compartmental models are used within a simulation or differential equation framework, primarily to predict the spread of the disease within the population (He et al., 2020; Mwalili et al., 2020; Iwata and Miyakoshi, 2020; Meltzer et al., 2014).

Decision support for resource allocation in preparedness, mitigation and control of infectious diseases is another important application domain for operation research and management science. However, similarly, the majority of the existing literature is based on simulation models or simulation-optimization frameworks, which do not explore the full range of decisions and control policies to guarantee that the optimal ones are selected (Dimitrov and Meyers, 2010).

Fewer studies considered compartmental models within mathematical optimization, such as linear, integer, non-linear, stochastic programming or optimal control, for decision making in preparing against and controlling infectious diseases. Sun et al. (2014) proposed linear optimization models for patient and resource allocation among hospitals in a health-care system during a pandemic influenza outbreak. Yarmand et al. (2014) proposed a two-stage stochastic linear program to optimally allocate vaccines

within a two-phase vaccination policy to contain an epidemic. Rachaniotis et al. (2012) proposed a theoretical analysis to derive decision support insights on mass vaccination against AH1N1 influenza pandemic. Büyüktahtakın et al. (2018) presented an epidemics-logistics mixed-integer linear optimization framework for determining optimal intervention strategies in terms of treatment capacities and location for controlling the Ebola epidemic. Their proposed model is interesting in that it combines a number of important features within the optimization framework, such as spatially varying rates for disease transmission and the migration of population among regions, which are also considered in this work together with a number of additional important improvements. More recently, Madubueze et al. (2020) studied the effect of different control strategies for the case of the COVID-19 pandemic, in particular quarantine and isolation, as time-dependent interventions using an optimal control approach.

The particular problem of allocating limited testing capacities and their impact on the dynamics of infectious disease is very rarely studied in the literature. Among the few studies we were able to identify is the work of Omondi et al. (2018) that develops a deterministic simulation model to provide a quantification of HIV prevention, testing and treatment in Kenya. More recently, the work of (Buhat et al., 2020) explores the optimal allocation of COVID-19 test kits among testing centers, but without considering an epidemiological model within the optimization problem and, instead, using historical data as demand points for estimating the need for testing kits; this makes the model of limited usage for deciding on future allocation decisions.

To the best of our knowledge, no existing study addresses the optimization problem of multi-region multi-period allocation of testing capacity to prepare against and control the spread of a pandemic. Our approach also differs in a number of ways from existing epidemiological resource allocation problems, among which, the explicit modeling of asymptomatic exposure and infection, the separation of distinct risk levels of infection for different segments of the population, and the consideration of an equity-based objective function to derive the allocation decisions. Finally, the MINLP model developed maintains the inherent non-linearity in pandemic progression dynamics, in particular with regards to the number of new infections and the positivity-rate of testing.

In summary, our research makes several distinct contributions to the literature:

i) The paper proposes a novel MINLP model based on an adapted compartmental SIR model for the optimal allocation of testing and control resources in a multi-spatial multi-temporal setting with the objective of minimizing the new infections in the population, as well as the cases that die without receiving hospitalization.

ii) The paper proposes novel extensions of the SIR compartmental model to take into account different levels of infection severity, asymptomatic transmission of the infectious disease, decisions related to testing symptomatic and asymptomatic individuals, case isolation modeling for confirmed cases and decisions related to hospitalization for severe cases, all within a single optimization framework.

iii) The paper proposes a novel formulation that considers the allocation of testing to asymptomatic and symptomatic individuals, and models the effect of positivity-rate of testing as a function of the ratio of the non-infected population to the total population.

iv) The paper considers an equity-driven objective function, based on the GINI index and weighed by

the population vulnerability level, to generate equitable testing allocation plans.

v) The proposed model is validated against real data for a case study of the COVID-19 outbreak in France, and the results are illustrated for a number of scenarios featuring realistic assumptions. The results provide insights on the impact of testing intervention time and level on the control of the pandemic. Moreover, the results confirm the usefulness of the proposed tool to help inform the policymakers on the level of preparedness needed in terms of testing capacity to control a large scale disease outbreak.

3. Pandemic progression and resource allocation model

The proposed model describes the diffusion of the virus as a state transition among 12 compartments in each physical location and for each time period, as illustrated in Fig. (1). In the Figure, the nodes represent the states of the individuals in the population impacted by the COVID-19 virus and the arcs represent the transition paths from one state to another, with the transition rate noted next to each arc. The state evolution of the population is either disease-dependent/clinical (solid arcs) or decision-dependent (dashed arcs).

The disease-dependent state progression is separated in two groups. The first group (grey) starts with the untested susceptible individuals ($\overline{NA}$), who become infected with transmission rates (σ_x^A, σ_x^B, σ_x^C) through community interactions with different infected subgroups and move to the untested-infected population ($\overline{IA}$, $\overline{ISM}$, $\overline{ISS}$), as a consequence of these interactions. Within the infected subgroups, individuals progress through several disease severity states: from asymptomatic to mildly-symptomatic to severely-symptomatic ($\overline{IA} \rightarrow \overline{ISM} \rightarrow \overline{ISS}$) with transition rates (μ_x and κ_x), respectively. The same transitions occur within the second group (red), which represents the same severity levels of infection, but for *tested and confirmed* individuals who have been identified and isolated ($\widetilde{IA}$, $\widetilde{ISM}$, $\widetilde{ISS}$) and, therefore, can no longer infect others. Infected individuals from both groups can, also, transition to recovery if they have mild symptoms ($\overline{ISM}$, $\widetilde{ISM} \rightarrow$ to R), with rates (ω_x^A), or to death if they have severe symptoms ($\overline{ISS}$, $\widetilde{ISS} \rightarrow D$), with rates ($\xi_x^A$).

The decision-dependent state progression concerns the testing and hospitalization states. If available capacities exist, asymptomatic and mildly-symptomatic individuals can get tested (TA and TS, respectively) and move to the respective identified state. Similarly, based on available capacities, severely symptomatic individuals can either be accepted to hospitals (H) or die without hospitalization. The formulation of the model is discussed in details in the following section.

3.1. Model notations

Sets and indices:

j	Index of time period.
$x \setminus y$	Indices of location.
J	Set of time periods.
X	Set of locations.
$Ny_{(x)}$	Set of surrounding locations to location x.
Ω	Set of connected locations.

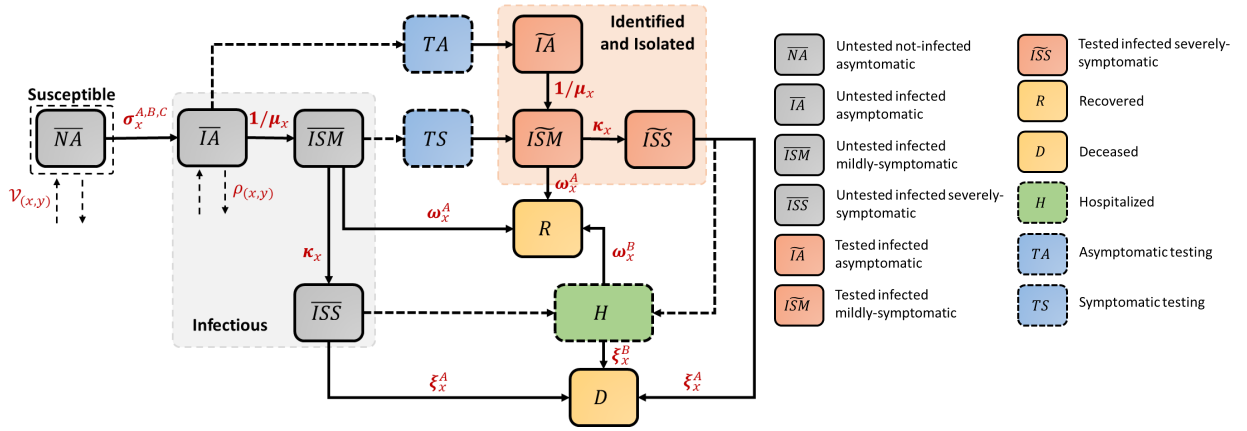

Figure 1: Proposed epidomological model framework including testing, hospitalization and quarantine measures

Disease transition parameters:

$\sigma_x^A \setminus \sigma_x^B \setminus \sigma_x^C$	Transmission rate of the disease due to community interaction with asymptomatic \ mildly symptomatic \ severely symptomatic individuals at location x.
ω_x^A	Transition rate of untested mildly symptomatic individuals who recover without hospitalization at location x.
ω_x^B	Transition rate of individuals who recover after being hospitalized at location x.
μ_x	Average time from infection to showing symptoms at location x.
κ_x	Transition rate from being mildly symptomatic to developing severe symptoms at location x.
ξ_x^A	Transition rate of severely symptomatic individuals who die without being hospitalized at location x.
ξ_x^B	Transition rate of severely symptomatic individuals who die after being hospitalized at location x.

Various model parameters:

$\mathcal{V}_{(x,y)} \setminus \rho_{(x,y)}$	Migration rate of non-infected asymptomatic\ infected asymptomatic individuals between location x and surrounding locations y.
$B^T \setminus B^H$	Total available testing \ hospitalization capacities.
TC_x^0	Existing testing capacity at location x at the beginning of the planning horizon.
$\mathcal{TP}_x$	Total population at location x.
$HC_{x,j}$	Total hospitalization capacity at location x time period j.
$\mathcal{IC}_x^*$	Initial condition of variable $*$ at location x.
ϑ_x	Normalized vulnerability score of location x.
$\mathcal{G}$	GINI coefficient expressed as a weighed measure of absolute differences.

State variables:

$\overline{NA}_{x,j} \setminus \overline{NS}_{x,j}$	Number of untested non-infected asymptomatic \ symptomatic individuals at location x at time j.
$\overline{IA}_{x,j} \setminus \overline{ISM}_{x,j} \setminus \overline{ISS}_{x,j}$	Number of untested infected asymptomatic \ mildly-symptomatic \ severely-symptomatic individuals at location x time j.
$\widetilde{IA}_{x,j} \setminus \widetilde{ISM}_{x,j} \setminus \widetilde{ISS}_{x,j}$	Number of tested infected asymptomatic \ mildly-symptomatic \ severely-symptomatic individuals at location x at time j.

$\overline{NA}^{[mob]}_{(x,y),j} \setminus \overline{IA}^{[mob]}_{(x,y),j}$	Number of non-infected \ infected asymptomatic individuals moving from location x to y at time j.
$H_{x,j} \setminus R_{x,j} \setminus D_{x,j}$	Number of hospitalized \ recovered \ deceased individuals at location x at time j
$TA_{x,j} \setminus TS_{x,j}$	Number of asymptomatic \ symptomatic individuals being tested at location x at time j.

Decision variables:

$\overline{A}^{[TA]}_{x,j} \setminus \overline{S}^{[TS]}_{x,j}$	Total Asymptomatic \ Symptomatic individuals both infected and non-infected accepted for testing at location x time period j.
$\overline{IA}^{[TA]}_{x,j} \setminus \overline{ISM}^{[TS]}_{x,j}$	Number of Infected Asymptomatic \ Symptomatic individuals accepted for testing at location x time period j.
$\overline{ISS}^{[H]}_{x,j} \setminus \widetilde{ISS}^{[H]}_{x,j}$	Number of untested \ tested and Infected Severely Symptomatic individuals accepted to be hospitalized at location x time period j.
$TC^{new}_{x,j} \setminus TC_{x,j}$	New \ Total testing capacity allocated to location x time period j.

3.2. Formulation of the MINLP optimization model for pandemic preparedness

3.2.1. Pandemic model objective function

The optimization seeks to minimize (Eq. 1): (i) the total number of newly infected individuals showing various severity levels of symptoms (asymptomatic, mildly symptomatic and severely symptomatic) and (ii) the number of deaths of infected individuals who do not get hospital treatment, for all locations and over the whole time horizon:

$$\begin{aligned}\min \sum_{x\in X}\sum_{j\in J}\left(\sigma^A_x\overline{IA}_{x,j}+\sigma^B_x\overline{ISM}_{x,j}+\sigma^C_x\overline{ISS}_{x,j}\right)\cdot\left(\frac{\overline{NA}_{x,j}}{\mathcal{TP}_x}\right)+\\ \sum_{x\in X}\sum_{j\in J}\xi^A_x\cdot\left(\left(\overline{ISS}_{x,j}-\overline{ISS}^{[H]}_{x,j}\right)+\left(\widetilde{ISS}_{x,j}-\widetilde{ISS}^{[H]}_{x,j}\right)\right)\end{aligned} \tag{1}$$

As can be seen in Eq. (1), the calculation of newly infected individuals results in a non-linear term in the objective function, that is a function of the disease transmission rates through the community interaction with infected individuals within the $\overline{IA}$, $\overline{ISM}$ and $\overline{ISS}$ populations at the end of period j, and the ratio of the remainder susceptible population in the region.

3.2.2. Pandemic transmission dynamics

Initial condition

The set of constraints, grouped in Eq. (2), define the initial conditions for the number of individuals in each of the states at each location and at the first time period:

$$\begin{aligned}&\overline{NA}_{x,j}=\mathcal{IC}^{\overline{NA}}_x,\quad \overline{IA}_{x,j}=\mathcal{IC}^{\overline{IA}}_x,\quad \overline{ISM}_{x,j}=\mathcal{IC}^{\overline{ISM}}_x,\quad \overline{ISS}_{x,j}=\mathcal{IC}^{\overline{ISS}}_x\\ &TA_{x,j}=\mathcal{IC}^{TA}_x,\quad TS_{x,j}=\mathcal{IC}^{TS}_x,\quad \widetilde{IA}_{x,j}=\mathcal{IC}^{\widetilde{IA}}_x,\quad \widetilde{ISM}_{x,j}=\mathcal{IC}^{\widetilde{ISM}}_x,\quad \widetilde{ISS}_{x,j}=\mathcal{IC}^{\widetilde{ISS}}_x\\ &H_{x,j}=\mathcal{IC}^{H}_x,\quad R_{x,j}=\mathcal{IC}^{R}_x,\quad D_{x,j}=\mathcal{IC}^{D}_x,\quad \forall x\in X, j=1\end{aligned} \tag{2}$$

Regional mobility constraints

It is important to consider the movement of the population between regions, as this impacts the disease transmission rates in the different regions. In this work, it is reasonably assumed that only *asymptomatic*

individuals remain mobile between regions during a pandemic outbreak and that symptomatic individuals remain confined in their respective regions until recovered (or in the worst-case deceased). It should be noted, however, that the asymptomatic population still contains infected individuals that may expose others to the disease and, therefore, may highly alter the infection rates between the regions (Moghadas et al., 2020).

The mobility of the non-infected asymptomatic individuals is described in Eq. (3) as the product of the mobility ratio $\mathcal{V}$ from region x to the connected regions y, and the number of non-infected asymptomatic individuals at each region x and time j. Similarly, the mobility of the infected asymptomatic individuals is formulated as the product of the mobility ratio ρ from region x to connected regions y, and the number of infected asymptomatic individuals at each region x and time j, as shown in Eq. (4):

$$\overline{NA}^{[mob]}_{(x,y),j} = \mathcal{V}_{(x,y)} \cdot \overline{NA}_{x,j}, \forall j \in J, (x,y) \in \Omega \tag{3}$$

$$\overline{IA}^{[mob]}_{(x,y),j} = \rho_{(x,y)} \cdot \overline{IA}_{x,j}, \forall j \in J, (x,y) \in \Omega \tag{4}$$

Notice that this formulation allows the direct implementation of different mobility policies, such as lock-downs, where mobility is restricted for some regions, by the proper setting of the mobility parameters ($\mathcal{V}$ and ρ).

Susceptible individuals

Constraints: constraint (5) defines the number of susceptible individuals (non-infected asymptomatic $\overline{NA}$ individuals) at the end of period $j+1$ to be equal to the number of susceptible individuals in the population in the previous period, plus the inwards-mobility to region x, minus the outwards-mobility from region x to connected regions y, minus newly infected individuals:

$$\begin{aligned}\overline{NA}_{x,j+1} = \overline{NA}_{x,j} + \sum_{y \in Ny_{(x)}} \overline{NA}^{[mob]}_{(y,x),j} - \sum_{y \in Ny_{(x)}} \overline{NA}^{[mob]}_{(x,y),j} \\ - \left(\sigma^A_x \overline{IA}_{x,j} - \sigma^B_x \overline{ISM}_{x,j} - \sigma^C_x \overline{ISS}_{x,j}\right) \cdot \left(\frac{\overline{NA}_{x,j}}{\mathcal{TP}_x}\right), \forall x \in X, j \in J\end{aligned} \tag{5}$$

Infectious individuals

Constraint (6) describes the number of untested infected asymptomatic individuals ($\overline{IA}$) at the end of period $j+1$ to be equal to the number of $\overline{IA}$ in the previous period, plus the inwards-mobility from surrounding regions to location x of individuals with similar state, minus the outwards-mobility from location x, minus $\overline{IA}$ individuals accepted for testing ($\overline{IA}^{[TA]}$), minus the proportion of the $\overline{IA}$ population that transitions to the mildly-symptomatic state without getting tested, plus newly infected individuals due to community interactions, as described in Eq (5):

$$\begin{aligned}\overline{IA}_{x,j+1} = \overline{IA}_{x,j} + \sum_{y \in Ny_{(x)}} \overline{IA}^{[mob]}_{(y,x),j} - \sum_{y \in Ny_{(x)}} \overline{IA}^{[mob]}_{(x,y),j} - \overline{IA}^{[TA]}_{x,j} - \frac{1}{\mu_x}\left(\overline{IA}_{x,j} - \overline{IA}^{[TA]}_{x,j}\right) \\ + \left(\sigma^A_x \overline{IA}_{x,j} + \sigma^B_x \overline{ISM}_{x,j} + \sigma^C_x \overline{ISS}_{x,j}\right) \cdot \left(\frac{\overline{NA}_{x,j}}{\mathcal{TP}_x}\right), \forall x \in X, j \in J\end{aligned} \tag{6}$$

Testing *asymptomatic* individuals, as is reflected in Eq (6), may be observed within a policy context

such as *contact tracing* (Braithwaite et al., 2020; Park et al., 2020; MacIntyre, 2020) or other specific policy implemented by the policymaker, which might impact the disease transmission dynamics.

Constraint (7) describes the number of untested infected mildly symptomatic individuals ($\overline{ISM}$) at the end of period $j+1$ to be equal to the number of $\overline{ISM}$ in the previous period, plus the proportion of the $\overline{IA}$ population that transitions to the $\overline{ISM}$ state, minus the number of $\overline{ISM}$ individuals that are accepted for testing, minus the remainder of the $\overline{ISM}$ population that either recovers (with transition rate ω^A) or develops severe symptoms (with transition rate κ):

$$\begin{aligned}\overline{ISM}_{x,j+1} = \overline{ISM}_{x,j} + \frac{1}{\mu_x}\left(\overline{IA}_{x,j} - \overline{IA}^{[TA]}_{x,j}\right) - \overline{ISM}^{[TS]}_{x,j} \\ - \left(\omega^A_x + \kappa_x\right)\left(\overline{ISM}_{x,j} - \overline{ISM}^{[TS]}_{x,j}\right), \forall x \in X, j \in J\end{aligned} \tag{7}$$

Symptomatic individuals are the primary candidates for testing and isolation measures. However, as will be described in Section 3.4), it is important to consider the positive rate of testing, since there exists a possibility of testing individuals showing or reporting similar symptoms and not actually having the disease.

Constraint (8) describes the number of untested infected severely symptomatic individuals ($\overline{ISS}$) at the end of period $j+1$, equal to the number of $\overline{ISS}$ in the previous period, plus the proportion of the $\overline{ISM}$ population that develops severe symptoms, minus the number of $\overline{ISM}$ individuals that are accepted for hospitalization ($\overline{ISS}^{[H]}$), minus the remainder of the $\overline{ISS}$ population that dies without being hospitalized due to lack of hospitalization resources, with transition rate ξ^A:

$$\begin{aligned}\overline{ISS}_{x,j+1} = \overline{ISS}_{x,j} + \kappa_x\left(\overline{ISM}_{x,j} - \overline{ISM}^{[TS]}_{x,j}\right) - \overline{ISS}^{[H]}_{x,j} \\ - \xi^A_x\left(\overline{ISS}_{x,j} - \overline{ISS}^{[H]}_{x,j}\right), \forall x \in X, j \in J\end{aligned} \tag{8}$$

Notice that testing decisions for the symptomatic population do not consider those individuals in the severely symptomatic state. This is because it is assumed that severely symptomatic individuals require specialized care (through hospitalization) regardless of whether they have been tested and confirmed, or not.

Infectious individuals (tested and confirmed)

Regarding the tested population: constraint (9) describes the number of tested infected asymptomatic individuals ($\widetilde{IA}$) at the end of period $j+1$, equal to the number of $\widetilde{IA}$ in the previous period, plus newly tested and confirmed individuals who were asymptomatic ($TA_{x,j}$) and minus the $\widetilde{IA}$ population that develops mild symptoms and transitions to the $\widetilde{ISM}$ state:

$$\widetilde{IA}_{x,j+1} = \widetilde{IA}_{x,j} + TA_{x,j} - \frac{1}{\mu_x}\widetilde{IA}_{x,j}, \quad \forall x \in X, j \in J \tag{9}$$

Constraint (10) describes the number of tested infected mildly symptomatic individuals ($\widetilde{ISM}$) at the end of period $j+1$, equal to the number of $\widetilde{ISM}$ in the previous period, plus newly tested and confirmed individuals from the symptomatic population, plus the proportion of the $\widetilde{IA}$ population that develops mild symptoms, minus the proportion of the $\widetilde{ISM}$ population that recovers (with transition rate ω^A), or

develops severe symptoms, with transition rate κ:

$$\widetilde{ISM}_{x,j+1} = \widetilde{ISM}_{x,j} + TS_{x,j} + \frac{1}{\mu_x}\widetilde{IA}_{x,j} - \kappa_x \widetilde{ISM}_{x,j} - \omega_x^A \widetilde{ISM}_{x,j}, \forall x \in X, j \in J \tag{10}$$

Constraint (11) describes the number of tested infected severely symptomatic individuals ($\widetilde{ISS}$) at the end of period $j+1$, equal to the number of $\widetilde{ISS}$ in the previous period, plus the proportion of the $\widetilde{ISM}$ population that develops severe symptoms, minus the number of $\widetilde{ISM}$ individuals that is accepted for hospitalization ($\widetilde{ISS}^{[H]}$), minus the remainder of the $\widetilde{ISS}$ population that dies without being hospitalized due to the lack in hospitalization resources, with transition rate ξ^A:

$$\widetilde{ISS}_{x,j+1} = \widetilde{ISS}_{x,j} + \kappa_x \widetilde{ISM}_{x,j} - \widetilde{ISS}_{x,j}^{[H]} - \xi_x^A \left(\widetilde{ISS}_{x,j} - \widetilde{ISS}_{x,j}^{[H]} \right), \forall x \in X, j \in J \tag{11}$$

Testing

Constraints (12) and (13) describe the number of individuals in testing states at $j+1$, equal to the number of individuals accepted for testing at the previous time period j, both for asymptomatic (12) and symptomatic (13) cases:

$$TA_{x,j+1} = \overline{IA}_{x,j}^{[TA]}, \quad \forall x \in X, j \in J \tag{12}$$

$$TS_{x,j+1} = \overline{ISM}_{x,j}^{[TS]}, \quad \forall x \in X, j \in J \tag{13}$$

Hospitalized

Constraint (14) represents the total number of individuals hospitalized in location x at the end of period $j+1$, which is equal to the total hospitalized in period j plus severely symptomatic individuals (both untested and tested) accepted for hospitalization minus the proportion of hospitalized individuals who recover (with transition rate ω^B) or die (with transition rate ξ^B).

$$H_{x,j+1} = H_{x,j} + \widetilde{ISS}_{x,j}^{[H]} + \overline{ISS}_{x,j}^{[H]} - \left(\omega_x^B + \xi_x^B\right) H_{x,j} \tag{14}$$

Recovered

Constraint (15) provides the cumulative number of individuals in location x who recover with or without being hospitalized. The total number of recovered individuals at the end of period $j+1$ is equal to the recovered individuals in the previous period plus newly recovered individuals coming from $\overline{ISM}$, $\widetilde{ISM}$ or H:

$$R_{x,j+1} = R_{x,j} + \omega_x^A \left(\overline{ISM}_{x,j} - \overline{ISM}_{x,j}^{[TS]} \right) + \omega_x^A \widetilde{ISM}_{x,j} + \omega_x^B H_{x,j}, \quad \forall x \in X, j \in J \tag{15}$$

Deceased

Constraint (16) provides the cumulative number of individuals in location x who die with or without being hospitalized. The number of deceased individuals at the end of period $j+1$ is equal to the deceased

individuals in the previous period plus newly deceased individuals coming from $\overline{ISS}$, $\widetilde{ISS}$ or H:

$$D_{x,j+1} = D_{x,j} + \xi_x^B H_{x,j} + \xi_x^A \left(\overline{ISS}_{x,j} - \overline{ISS}_{x,j}^{[H]}\right) + \xi_x^A \left(\widetilde{ISS}_{x,j} - \widetilde{ISS}_{x,j}^{[H]}\right), \forall x \in X, j \in J \tag{16}$$

3.3. Resources allocation constraints (testing and hospitalization)

The resource allocation constraints that face the policymaker are presented in Eqs. (17)-(23). Decisions regarding the spatial and temporal management of limited testing and control as well as hospitalization resources, are simultaneously optimized within a single optimization model, under the conditions developed by the disease transmission dynamics defined by Eqs. (2)-(16).

Hospitalization limit

Constraint (17) limits the total number of individuals hospitalized to the number of available hospitalization capacity in location x at the end of period j. This is calculated as the minimum between the remaining capacity available to accommodate new severe cases at time j in location x ($HC_{x,j} - H_{x,j}$) and the total number of severely infected individuals requiring hospitalization ($\overline{ISS}$ and $\widetilde{ISS}$) if there is enough hospitalization resources:

$$\widetilde{ISS}_{x,j}^{[H]} + \overline{ISS}_{x,j}^{[H]} \leq \min\left\{\widetilde{ISS}_{x,j} + \overline{ISS}_{x,j}, HC_{x,j} - H_{x,j}\right\}, \forall x \in X, j \in J \tag{17}$$

$$H_{x,j} \leq HC_{x,j}, \quad \forall x \in X, j \in J \tag{18}$$

Testing limit

Constraint (19) limits the total number of individuals tested to the number of available testing resources in location x at the end of period j. This is calculated as the minimum between the remaining testing capacity available after accepting asymptomatic and symptomatic individuals for testing ($TC_{x,j} - (TA_{x,j} + TS_{x,j})$) and the total number of the asymptomatic and mildly symptomatic individuals ($\overline{IA} + \overline{ISM}$), if there is enough testing resources:

$$\overline{IA}_{x,j}^{[TA]} + \overline{ISM}_{x,j}^{[TS]} \leq \min\left\{\overline{IA}_{x,j} + \overline{ISM}_{x,j}, TC_{x,j} - (TA_{x,j} + TS_{x,j})\right\}, \forall x \in X, j \in J \tag{19}$$

$$TA_{x,j} + TS_{x,j} \leq TC_{x,j}, \quad \forall x \in X, j \in J \tag{20}$$

Allocation of testing capacity

Constraint (21) determines the total cumulative testing capacity available in location x up to period j, including any available initial testing resources TC^0:

$$TC_{x,j} = \sum_{\tau=\mathcal{I}^{start}}^{j} TC_{x,\tau}^{new} + TC_x^0, \forall x \in X, j \in J \setminus \bar{J} \tag{21}$$

Budget for allocating testing

Constraints (22) and (23) limit the total testing resources available for distribution to the maximum level B^T and ensure that testing capacities are available only at the start of the defined intervention date $\mathcal{I}^{start}$:

$$\sum_{x \in X} \sum_{j=\mathcal{I}^{start}}^{\bar{J}} TC_{x,j}^{new} \leq B^T \tag{22}$$

$$\sum_{x \in X} \sum_{j=1}^{\mathcal{I}^{start}} TC_{x,j}^{new} = 0 \tag{23}$$

Non-negativity and integrality

$$\text{All variables are non-negative,} \quad TC_{x,j}^{new} \; integer, \quad \forall x \in X, j \in J \tag{24}$$

3.4. Modeling the positivity-rate of testing

Notice how, according to the mathematical model introduced thus far, the positivity-rate of the testing results is not considered, leading to an assumption that 100% of the total tested individuals will be identified as infected. This is, evidently, not realistic: a high number of asymptomatic individuals who might be tested (because of contact tracing or other reasons) will not actually have the disease and, therefore, their test results will be negative. Similarly, a number of individuals showing similar symptoms might, in fact, have another illness and should, therefore, also test negative. This is what is referred to as the positivity-rate of testing and it should be properly taken into consideration in the disease transmission and management model.

In order to consider the positivity-rate of testing, we introduce two new variables $\overline{A}_{x,j}^{[TA]}$ and $\overline{S}_{x,j}^{[TS]}$ that serve to compute the *effective* number of infected asymptomatic and symptomatic individuals identified by testing, respectively. The following constraints are, therefore, added:

$$\overline{A}_{x,j}^{[TA]} + \overline{S}_{x,j}^{[TS]} <= TC_{x,j}, \forall x \in X, j \in J \tag{25a}$$

$$\overline{A}_{x,j}^{[TA]} \leq \overline{NA}_{x,j} + \overline{IA}_{x,j}, \forall x \in X, j \in J \tag{25b}$$

$$\overline{IA}_{x,j}^{[TA]} = \overline{A}_{x,j}^{[TA]} \cdot \frac{\overline{IA}_{x,j}}{\overline{NA}_{x,j} + \overline{IA}_{x,j}}, \forall x \in X, j \in J \tag{25c}$$

$$\overline{S}_{x,j}^{[TS]} \leq \overline{NS}_{x,j} + \overline{ISM}_{x,j}, \forall x \in X, j \in J \tag{25d}$$

$$\overline{ISM}_{x,j}^{[TS]} = \overline{S}_{x,j}^{[TS]} \cdot \frac{\overline{ISM}_{x,j}}{\overline{NS}_{x,j} + \overline{ISM}_{x,j}}, \forall x \in X, j \in J \tag{25e}$$

Eq. (25a) ensures that the number of tests conducted on asymptomatic and symptomatic individuals is limited by the total tests capacity. Eq. (25b) limits the number of tests conducted on asymptomatic individuals by the total asymptomatic population size. Eq. (25c) relates the total asymptomatic tests with its resulting number of positive cases by the positivity rate $\frac{\overline{IA}_{x,j}}{\overline{NA}_{x,j}+\overline{IA}_{x,j}}$, which is the fraction of infected asymptomatic individuals over the total asymptomatic population. Eq. (25d) enforces that the number of tests conducted on (mild) symptomatic individuals is limited by the total mild symptomatic population size. Eq. (25e) relates the total symptomatic testings with its resulting number of positive cases by the positivity rate $\frac{\overline{ISM}_{x,j}}{\overline{NS}_{x,j}+\overline{ISM}_{x,j}}$, where $\overline{NS}$ represents the population that shows similar symptoms but that is not infected by the specific disease.

Notice that, the objective function (1) and constraints (5), (6), (25c) and (25e) are non-convex and nonlinear. The resulting model described by Eqs. (1)-(25e) is, therefore, a Mixed Integer Non-Linear Program (MINLP).

4. Generating Equitable Resource Allocation Plans

For ease of discussion, let us define the previously formulated objective function for each region and each time step (1) to be:

$$\mathcal{O}_{x,j} = \left(\sigma_x^A \overline{IA}_{x,j} + \sigma_x^B \overline{ISM}_{x,j} + \sigma_x^C \overline{ISS}_{x,j}\right) \cdot \left(\frac{\overline{NA}_{x,j}}{\mathcal{TP}_x}\right) + \xi_x^A \cdot \left(\left(\overline{ISS}_{x,j} - \overline{ISS}_{x,j}^{[H]}\right) + \left(\widetilde{ISS}_{x,j} - \widetilde{ISS}_{x,j}^{[H]}\right)\right), \forall x \in X, j \in J \tag{26}$$

Generating equitable plans require adapting the objective function to consider an equity measure between the various regions among which the resources are to be allocated. The measure $\mathcal{O}_{x,j}$ is the total number of infected individuals that remain untested and those who die without receiving hospitalization. We complement this measure with an equity measure $\mathcal{G}$, the Gini coefficient, which is a popular measure of inequity. To formulate the equity-driven objective function we follow the rationale developed in Eisenhandler and Tzur (2018), wherein the objective function balances two fundamental principles of public management, effectiveness and equity. To achieve this, the equity-based objective function is defined as:

$$\min_{\Xi} \sum_{x \in X} \sum_{j \in J} \mathcal{O}_{x,j}(1 + \mathcal{G}) \tag{27}$$

where the GINI index $\mathcal{G}$ is measuring the weighed absolute difference in the allocation policy of two regions:

$$\mathcal{G} = \frac{\sum_{x \in X} \sum_{x' \in X : x' > x} \left| \vartheta_{x'} \sum_{j \in J} \mathcal{O}_{x,j} - \vartheta_x \sum_{j \in J} \mathcal{O}_{x',j} \right|}{\sum_{x \in X} \sum_{j \in J} \mathcal{O}_{x,j}}, \tag{28}$$

and the weight ϑ_x reflects the importance of each individual region, understood here as the vulnerability level of each region x. This leads to the following easily linearizable objective function:

$$\min_{\Xi} \left\{ \sum_{x \in X} \sum_{j \in J} \mathcal{O}_{x,j} + \sum_{x \in X} \sum_{x' \in X : x' > x} \left| \vartheta_{x'} \sum_{j \in J} \mathcal{O}_{x,j} - \vartheta_x \sum_{j \in J} \mathcal{O}_{x',j} \right| \right\} \tag{29}$$

ϑ_x can be calculated based on any number of vulnerability factors associated with region x. These factors are typically related to physical, social, economic, and/or environmental vulnerability indicators. For example, factors such as unemployment rate, poverty level or the proportion of physically vulnerable individuals in the population may be used to calculate the level ϑ_x. However, socio-economic criteria for allocating health-related resources may be difficult to validate and may often lead to controversial outcomes. In this study, we propose to calculate a vulnerability score based on a vulnerability factor which is the number of available hospital beds per capita in the respected region (Ministère des solidarités et de la santé , 2020). A discussion on the choice of this vulnerability factor and its validation can be found in Appendix B.

The normalized vulnerability score for each region x, is calculated as follows:

$$\vartheta_x = \frac{\eta_x / \mathcal{TP}_x}{\sum_{x \in X} (\eta_x / \mathcal{TP}_x)}, \ \forall x \in X \tag{30}$$

in which (η_x) is the selected vulnerability factor and $(\mathcal{TP}_x)$ is the population size of each region.

5. Case study

The MINLP optimization model for pandemic preparedness introduced in Section 3.2 is applied to the real case study of the COVID-19 pandemic outbreak in France. To illustrate the usefulness of the model on a real application for the allocation of limited testing and control resources, a case study covering 3 interconnected regions in France is considered. Administratively, France is composed of 13 metropolitan regions as well as 5 overseas regions. The case study considers 3 of the major metropolitan regions, namely: i) Ile-de-France (IdF): the most populous region and where the capital is located, ii) Grand-Est (GE): one of the regions that were significantly impacted by the early spread of the disease and, iii) Centre-Val de Loire (CVdL): a region which borders the most with regions in metropolitan France and may, therefore, be considered as an important connecting hub for the different regions. The choice of the geographical level (regional, country level, cities, etc.), as well as the number of regions considered in the case study, is primarily done to ensure the consistency of the data sources used as well as the clarity of evaluating and discussing the results obtained. The model, as formulated, can straightforwardly accommodate different geographical levels and numbers of locations as needed.

France is reportedly the first country in Europe where COVID-19 cases were imported (ECDC, 2020). At the time of writing, the number of confirmed cases and the number of deaths related to the COVID-19 infection in France have reached levels higher than 2.5 million cases and 60 thousand deaths (WHO et al., 2020). For the case study, we focus our attention on leveraging the MINLP model developed in this work to optimally allocate the available testing capacities among the different regions in France, with the objective of achieving the minimal number of new infections and of deaths of individuals who do not receive medical attention.

The data used for the numerical analysis includes disease transition parameters (Table 4), population and geographic data (Table 5) and data describing the mobility of population between regions collected on a departmental level and aggregated for each region, as shown in Figure 2 (Table 6). The disease transition parameters are described in Table 4 and are calculated based on clinical progression models (column 3) and generally known clinical values of the Covid-19 virus (column 4). These values are largely based on the sources cited in the Table. An exception to that are the transmission rates from susceptible to infected individuals (σ), which depend on location-specific attributes, such as the local policy implemented (confinement, travel bans, social distancing or other measures), the behavior of the population with regards to those policies (Rajaonah and Zio, 2020) as well as other local factors. These values, therefore, need to be estimated or collected for the specific regions studied and under particular policy periods. In this study, we calibrate these values to reflect the disease transmission characteristics for Ile-de-France during the first de-confinement period (between the 1st of June to the 31st of October) and we ensure that the model results are validated for all other regions and under a variety of indicators. The model validation is thoroughly discussed in Section (6.1).

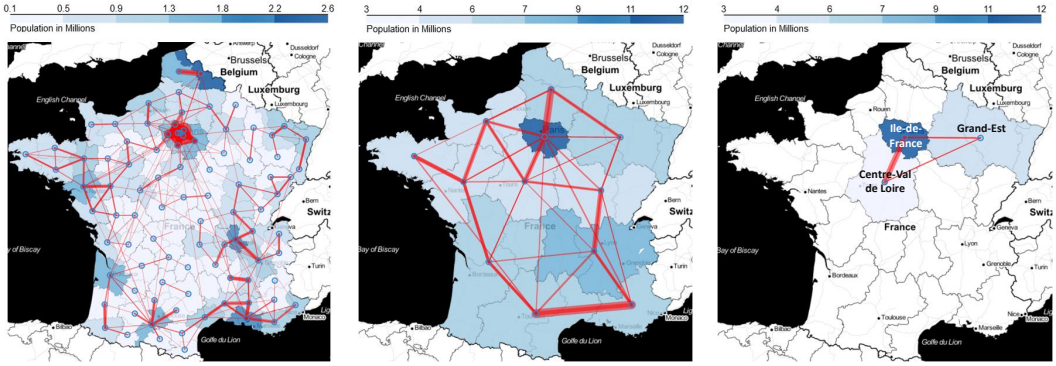

(a) Mobility per department **(b)** Mobility per region **(c)** Mobility between regions selected for the case-study

Figure 2: Average daily mobility within departments and regions in France.

Table (5) summarizes information about the population size and information about the available hospitalization resources in each region (total number of beds in intensive care, reanimation and continuous care units) (Ministère des solidarités et de la santé , 2020). An important data vector is the initial number of infected individuals in the population at the start of the planning horizon. The number of infected individuals per region is very difficult to know at the outbreak of a pandemic or without universal testing of all individuals; yet, it is important to initialize these numbers for the model state transitions to occur. We assume a relatively low number of initial infections per region in proportion to the population size and note that the only impact of varying these estimates is to shift the output along the time axis (high number of initial infections lead to earlier infections or deaths peaks, and low number of initial infections lead to delayed infections or death peaks (Duffey and Zio, 2020)) while preserving the exact transition proportions. This means that any conclusion on the results holds for any initialization of the parameters, with the exception of the observation time of occurrence. Finally, Table (6) summarizes the daily net movement between regions aggregated across all age segments and different traveling motivations, in particular work and study; the data have been obtained from (INSEE, 2019a,b).

The case studies consider daily progression and planning for the pandemic, in terms of allocation of testing resources under different resource availability levels and intervention start dates. Except for the choices related to the model validation illustrated in the next section; the analysis spans a horizon of 210 days (7 months) to allow for a planning comparison of a reasonably long period in which the decisions are relevant, and not too long that new information impact the model parameters initialization.

6. Results and Analysis

In this section, we present the model validation and discuss its results with respect to actual data obtained for the selected regions. We, then, proceed to illustrate and analyze the results of optimal resource allocation obtained by the model under a variety of intervention levels and starting dates. All the solutions presented are obtained by solving the MINLP model (2)-(24), (25a)-(25e) with the standard objective function in Eq. (1) denoted ($\mathcal{O}$) and, then, with the equity-driven objective Eq. (29) defined in Section 4, and denoted ($\mathcal{O}_{Equity}$). The non-linear model is solved using the Interior Point Optimizer (IPOPT) solver (Wächter and Biegler, 2006), along with the HSL_MA97 sparse direct solver (Hogg and

Table 4: Disease transition parameters.

Parameter	Description	SARS-COV-2 Clinical Progression	Estimated clinical value	Source
$\frac{1}{\mu}$	Progression rate from exposed to symptomatic class	μ = Incubation period of the disease (5 days)	0.2	(Lauer et al., 2020; Linton et al., 2020; Wassie et al., 2020)
ω_A	Recovery rate for mild cases	$\frac{\omega_A}{\omega_A+\kappa}$ = Proportion of mild infections ($\approx 77\%$)	0.15	(Wu and McGoogan, 2020; Pan et al., 2020)
ω_B	Recovery rate for severe cases (hospitalized)	$\frac{\xi_B}{\omega_B+\xi_B}\cdot\frac{\kappa}{\omega_A+\kappa}$ = Case fatality ratio ($\approx 2.6\%$)	0.08	(Wu and McGoogan, 2020; Dong et al., 2020; Russell et al., 2020; Öztoprak and Javed, 2020)
κ	Progression rate from mild to severe symptomatic class	$\frac{1}{\omega_A+\kappa}$ = Duration of mild symptoms ($\approx$ 5.3 days)	0.038	(Wölfel et al., 2020; Li et al., 2020)
ξ_A	Death rate for non-hospitalized severe cases	$\frac{1}{\xi_A}$ = Duration of severe symptoms ($\approx$ 14 days)	0.07	(Linton et al., 2020; Zhou et al., 2020)
ξ_B	Death rate for hospitalized severe cases	$\frac{1}{\omega_B+\xi_B}$ = Duration of ICU stay ($\approx$ 10 days)	0.012	(Zhou et al., 2020; Ferguson et al., 2020)
σ	Transmission rate from susceptible to infected	$\sigma = \sigma_A\cdot\overline{IA}+\sigma_B\cdot\overline{ISM}+\sigma_C\cdot\overline{ISS}$	σ_A=0.21 σ_B=0.115 σ_C=0.06	(Calibrated for the disease progression in France. Further discussed in Section 6.1)

Table 5: Population and regional specific data.

	Ile-de-France (IdF)	Centre-Val de Loire (CVdL)	Grand-Est (GE)
Population size	12,278,210	2,559,073	5,511,747
Total number of hospital beds available (Ministère des solidarités et de la santé , 2020)	3,951	757	1,707
Estimated hospital occupancy level at the beginning of the modeling horizon (approximated based on hospitalization data available prior to chosen start date (Santé publique France, 2020a))	65%	40%	85%
Estimated number of initial infections (assumed in proportion to the population size)	100	10	15

Scott, 2011), which is capable of handling large-sized instances. To handle the numerical complexity and stability of the non-linear model, the problem for each region is first solved independently and, then, the obtained solutions are used to warm-start the solver for the interconnected regional problem considering the movement of susceptible and infected populations between regions. All solutions reported are obtained by solving to optimality on a desktop computer running LINUX OS with 12 cores, 3.2 GHz CPU and 32 gigabyte memory. All solutions were obtained within approximately 600 seconds of run time.

6.1. Model validation

To ensure that the proposed MINLP model is adequately capable of informing the pandemic preparedness decisions, the model is validated against the current pandemic outbreak data in France to accurately predict the real pandemic progression, given the formulation and the parameters settings. The model is validated by fixing the values of the decision variables for the daily number of tests con-

Table 6: Inter-regional mobility data.

From	To	Daily Net Movement (in number of individuals). Source: (INSEE, 2019a,b)
Ile-de-France (IdF)	Centre-Val de Loire (CVdL)	3,942
Ile-de-France (IdF)	Grand-Est (GE)	400
Centre-Val de Loire (CVdL)	Grand-Est (GE)	225

ducted per region ($TS_{x,j} + TA_{x,j}$) and the daily hospitalization ($H_{x,j}$) to the actual data observed for the region during a particular period and, then, solving the model to ensure that the observed disease state transition variables, such as the number of daily confirmed cases in each region, the daily cumulative number of deaths in each region and the daily number of positivity rate of testing per region, match the actual data. To achieve this, the regional specific parameter (σ) for the disease transmission between the different infections levels is first calibrated for one region and one output (in this case Ile-de-France, on the number of confirmed cases) and, then, the validation is performed as described. This means that the results for each region are validated on 3 different outputs (number of confirmed cases, number of deaths and positivity-rates of testing), including the effect of interdependent mobility between regions, leading to a validation that is expected to adequately cover the modeling choices and parameters settings.

The choice of the time period selected for validation is critical, as different intervention policies have been applied to control the pandemic outbreak since its beginning. These measures include confinements, social-distancing and travel restrictions to different degrees in different periods. To ensure that the validation is consistent, the period chosen, therefore, should be consistent in the type of policies implemented and to the relevance of these policies. In this study, we chose to validate the model for the disease transmission under normal population movement (not under confinement) to ensure its relevance in a preparedness setting where no specific policies have been implemented. Ideally, this should be achieved using data from the onset of the pandemic outbreak, before any intervention measures have been implemented; however, these data are not clearly available for the Covid-19 pandemic, since most countries have implemented a confinement strategy very promptly at the onset of the outbreak.

In France, the first confinement lasted from the 17th of March to the 11th of May, and a second confinement started on the 30th of October. Therefore, for the model validation, we chose the outbreak data for the period from the 1st of June to the 30th of October for the three selected regions Ile-de-France (Idf), Centre-Val de Loire (CVdL) and Grand-Est (GE) during the deconfinement period. Graphical representations of the real data used on testing (Santé publique France, 2020b) and hospitalization (Santé publique France, 2020a) are shown in Appendix A.

Figure (3) provides a visual comparison between the actual pandemic progression data and the model results for the daily number of confirmed Covid-19 cases (Fig. 3a), the daily cumulative number of deaths (Fig. 3b) and the daily positivity-rate of testing (Fig. 3c), during the period between June 1st, 2020 and October 30, 2020 in Ile-de-France (Idf), Centre-Val de Loire (CVdL) and Grand-Est (GE). The visual comparison demonstrates that the proposed model provides a good fit for the daily number of cases and the daily level of positivity-rate of testing in all three regions. For the daily number of deaths, it is seen that, while overall the model results provide a good-fit, there is a slight underestimation of the number of cases for Ile-de-France and Grand-Est, and an overestimation for Centre-Val de la Loire in particular for

the cumulative number of deaths in the last two months of the studied period (September and October). It is reasonable to believe that a significant part of those misestimations is due to unreliability in data reported for the number of deaths, as it has been reported that in many instances those cases are reported with notable delays (Santé publique France, 2020a). It is noted, however, that the difference between the model output and the real data remains relatively low (the order of magnitude is in a few hundreds at most for the cumulative number of deaths as opposed to an order of magnitude of millions for the other indicators).

The goodness-of-fit of the model results is confirmed quantitatively by computing the normalized mean absolute deviation (nMAD), the normalized root mean squared error (nRMSE) and the Explained Variance between the actual data and the model results, as summarized in Table (7). It is shown that, with the exception of the number of deaths for CVdL discussed above, the error values (nMAD and nRMSE) are very low and the Explained Variance is significant, with the lowest value being around 0.8 (maximum 1). In addition, it is shown that, for the number of deaths in the CVdL region, the error measures are low for the first three months of the data reported, with the deviation being mostly towards the end, which we note to be possibly, again, due to errors in real data reporting.

Table 7: Model validation: assessment using different error metrics.

		Metric		
Region	**Data**	**nMAD**	**nRMSE**	**Explained Variance**
Ile-de-France	Infection	0.009	0.013	0.998
	Deaths	0.064	0.077	0.962
	Positivity-Rate	0.052	0.066	0.958
Centre-Val de Loire	Infection	0.023	0.044	0.958
	Deaths	**0.264**	**0.455**	**-2.111**
	Deaths (from 01/06 to 30/08)	**0.067**	**0.091**	**0.923**
	Positivity-Rate	0.075	0.107	0.797
Grand-Est	Infection	0.021	0.035	0.975
	Deaths	0.079	0.094	0.869
	Positivity-Rate	0.064	0.110	0.801

6.2. Optimal allocation of testing and control resources

In this section, the optimal decisions regarding the allocation of the available resources to control and minimize the impact of the pandemic is investigated. In particular, we focus on the allocation of testing resources and implementation of control measures, and their impact on reducing the progression of the disease transmission within the population, by properly identifying and isolating the infected cases. For this, the MINLP model proposed is solved for different scenarios of total available testing capacity and different intervention starting dates. We consider a mid-term planning period of 7 months (210 days) since, in most cases, it is reasonable to assume that the daily allocation decisions will need to be updated after a given time, in response to the disease progression. For the hospitalization capacities, the allocation are also optimally obtained in the model; however, we do not consider investments in new hospitalization capacities and, instead, consider the real hospitalization capacity known for each region, as previously reported in Table (2c). The planning of new hospital investments can be straightforwardly investigated using the proposed model, by varying the parameter B^H, in particular if longer planning periods are considered.

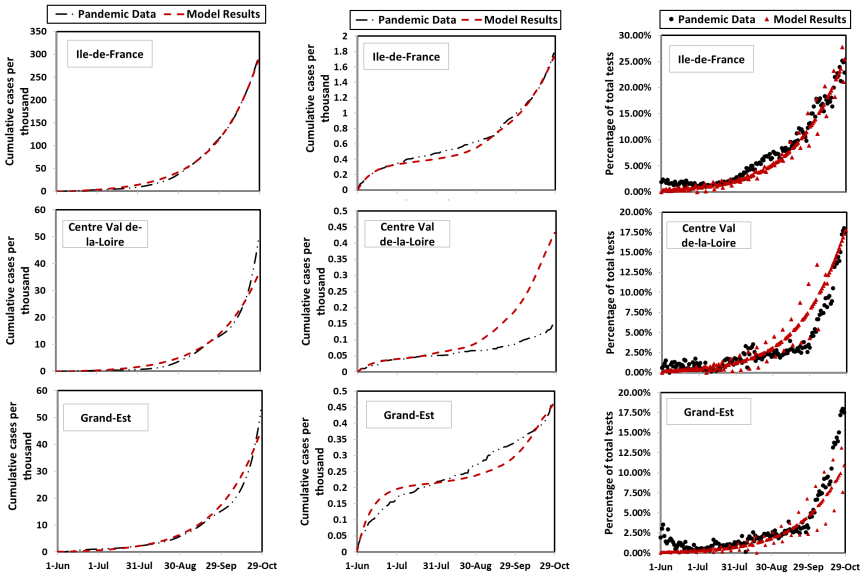

(a) Daily number of confirmed cases **(b)** Cumulative number of deaths **(c)** Daily level of positivity-rates of testing

Figure 3: Model validation: comparison between the actual pandemic data and the model results under the same hospitalization and testing levels.

6.2.1. Impact of the level of testing and control intervention on the pandemic progression

For a limited testing capacity, the MINLP model proposed seeks to allocate the testing resources optimally among the different regions to minimize the overall pandemic impact in terms of the number of infected and number of deceased individuals. In this section, we investigate the optimal allocation results for 5 intervention levels : no testing, 5000, 10000, 50000 and 100000 tests/day available to be distributed among all regions. Table (8) summarizes the optimal solution for allocating the available testing resources for each region and for all intervention levels. Table (8) also summarizes the impact of this optimal allocation and deployment of testing and control measures on the disease progression within the population, in terms of total number of infected individuals, total hospitalizations (limited by the available hospital capacities), cumulative deaths and recoveries.

As seen in Table (8), significant improvements are observed in terms of the number of people infected, hospitalized or deceased as the testing and control resources increase, regardless of the particular distribution among the regions. The "no testing" scenario performs considerably poor in terms of the total number of infected, hospitalized and deceased individuals. In this scenario, the number of infections in the population reaches more than 8M infections for IdF, 1.7M infections for CVdL and 3.6M infections for GE, which represent around 66.57%, 67.35% and 66.70% of the total population of IdF, CVdL and GE, respectively. Moreover, the results show that, in the absence of testing and control measures, around 3 million individuals in total (1.78M for IdF, 0.36M for CVdL and 0.77M for GE) are expected to die, as seen in Table (8). This represents a considerable 14% deaths of the population of each region. However, when testing and control interventions are introduced by increasing the total number of tests per day, the impact of the disease reduces considerably. Even by opting for the median scenario of 10,000 tests per day, the percentage of infections reduces to 2.2M, 290K and 471K, which represents 18%, 11% and 8% of

the population of IdF, CVdL and GE, respectively. Moreover, the number of deceased cases reduces to 112K, 12K and 18K, representing much lower percentages, i.e. 0.9%, 0.47% and 0.34% of the population of IdF, CVdL and GE, compared to the average of 14% deaths observed when no intervention occurs. These improvements continue as the number of daily tests deployed is increasing, infections reaching levels lower than 2% and deaths reaching levels lower than 0.06% when 100,000 total tests per day are optimally allocated and implemented.

The number of cases in hospitals reduces as more testing and control is introduced, although it maintains a lower improvement rate. This is because with limited hospitalization capacity, the maximum number of new daily hospital admissions cannot be surpassed until more places are vacated from patients under treatment. This results in hospitalization bottlenecks even if the number of severe cases requiring hospitalization are significantly reduced.

In terms of how the testing resources are allocated, Table 8 shows that in all scenarios with non-zero testing capacity, the majority of the available resources are allocated to the highly populated region IdF. This is reasonable as more community interactions, disease transmission and mobility in and out of the region occur as a result of the higher number of population and, therefore, more resources would be needed to effectively manage this region. Interestingly, while this logic also holds when considering the other regions, the results in terms of the resources distribution are not directly correlated to the population size. Indeed, while CVdL has the lowest population size, for the highest intervention level T = 100,000/day, the optimal solution is to allocate more resources to this region compared to the more populous GE. This may be explained due to the impact of mobility between regions, which affects how fast the disease transmits within a population.

Table 8: Optimal allocation of different testing capacities among regions and their impact on the disease transition dynamics.

Testing Capacity	Region	Testing capacity allocation	Infected	Hospitalized	Deaths	Recovered
No Testing	Ile-de-France (Idf)	0	8,173,957	52,820	1,779,454	6,352,735
	Centre-Val de Loire (CVdL)	0	1,723,590	9,713	361,077	1,303,597
	Grand-Est (GE)	0	3,676,528	21,184	770,795	2,827,246
T = 5,000/day	Ile-de-France (Idf)	1,509	7,984,253	47,742	1,633,359	6254462
	Centre-Val de Loire (CVdL)	702	1,652,017	7,495	225,145	1,089,777
	Grand-Est (GE)	2,790	542,707	11,111	21,130	222,373
T = 10,000/day	Ile-de-France (Idf)	6,436	2,268,596	32,163	112,132	1,039,089
	Centre-Val de Loire (CVdL)	1,225	290,292	5,472	12,092	123,760
	Grand-Est (GE)	2,338	471,932	11,276	18,985	207,509
T = 50,000/day	Ile-de-France (Idf)	41,461	319,833	29,077	15,490	204,374
	Centre-Val de Loire (CVdL)	3,309	54,435	4,946	2,171	32,658
	Grand-Est (GE)	5,230	75,140	9,050	2,181	48,000
T = 100,000/day	Ile-de-France (Idf)	87,929	199,423	25,253	6783	135,247
	Centre-Val de Loire (CVdL)	6,244	43,279	4,670	1,529	27,288
	Grand-Est (GE)	5,827	72,852	8,979	2,092	46,978

While the impact of increasing the testing and control interventions is significant in terms of reducing the total number of infections within the population, it is also interesting to investigate how the intervention may impact the progression time of the infections within the population. Fig. (4) illustrates the time series for the evolution of the disease infection level in each region and for each testing and control intervention level. It is seen that increasing the number of tests per day does not only reduce the total

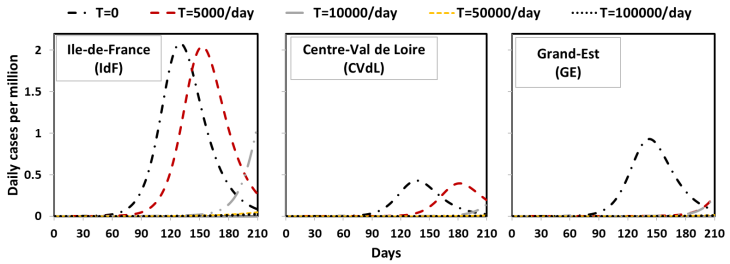

Figure 4: Time series for the daily number of total infections for each region and for every scenario of intervention level, over the whole planning horizon.

number of infections, but it also reduces the peak level of the infections and delays its occurrence as shown in Fig (4). This can be particularly important if scarce testing and control resources are available, to extend the time available to prepare other medical interventions or to decide on a policy intervention in order to mitigate the worst outcomes. Finally, notice that at high testing and control levels (above 10,000 tests per day), the new infection rates are very low, with no apparent peak during the studied horizon.

Similar results for the impact of increasing the testing and control measures on delaying the hospitals congestion can be seen in Fig. (5). Fig. (5) illustrates the time series for daily hospitals occupancy in each region and for each intervention level. It is shown that, for all intervention levels, the hospitals eventually become congested and operated at their full capacities (the converging horizontal lines in the Figures). However, reaching this maximum occupancy limit can be effectively delayed by a number of months, by increasing the testing and control resources and optimally allocating them between regions. For example, for IdF region, delays in reaching hospital capacity limits of 3,500 individuals receiving treatment at a given day is observed to be attained after around 4.5 months from the start of the pandemic for the scenario of T = 10,000 tests/day, compared to being reached only after 2 months for the scenario where no testing is introduced. This is even longer as the number of testing and control resources allocated increase and is observed for all regions, with hospitalization reaching their full capacity after 6 months for the highest testing intervention levels.

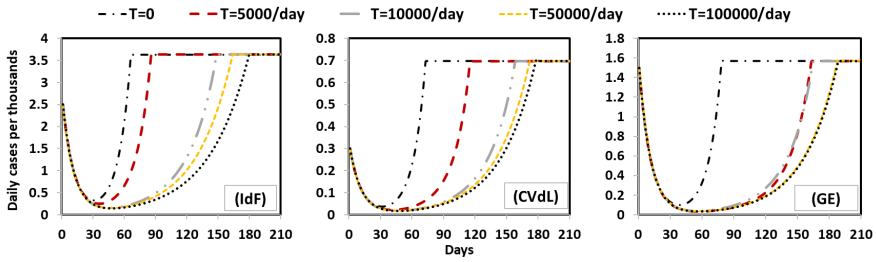

Figure 5: Time series for daily number of individuals receiving treatment in hospitals, for each region, for every testing and control level, over the whole planning horizon.

Finally, out of the available daily testing and control resources allocated per region, the proposed model is capable to inform the optimal allocation of testing between asymptomatic vs symptomatic individuals to ensure the most effective outcomes. These results are shown in Fig. (6) for the average number of individuals tested from each population (symptomatic vs asymptomatic), at each region and for each

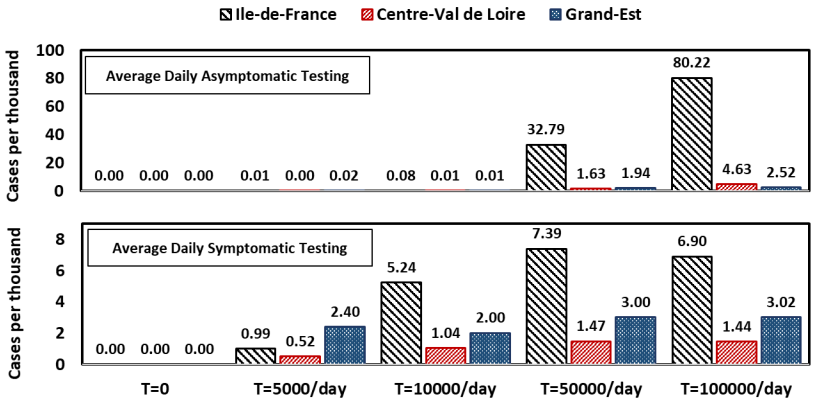

Figure 6: Comparison between the testing and control resource allocation among asymptomatic individuals and symptomatic individuals, for each region and for each intervention level.

intervention level considered. The results suggest that, for low intervention levels (T = 5000 tests/day and T = 10,000 tests/day) the model allocates almost all the testing resources to the *symptomatic* individuals in all three regions (IdF, CVdL and GE). However, as the number of available testing and control resources increase, a significant proportion is allocated to testing the *asymptomatic* population. These results are reasonable since, for a limited number of tests, it is more effective to control individuals already showing signs and not to waste any testing capacity on non-infected individuals, which is highly probable within the asymptomatic population.

6.2.2. Impact of the intervention time of testing and control measures on the pandemic progression in the selected regions

The results obtained in the previous section showed how the optimal allocation of testing and control resources lead to a significant reduction in the disease progression, the number of hospitalization and the number of deaths within the population. Moreover, different levels of resources availability was investigated and analyzed. Thus far, the investigation performed has assumed that the testing and control intervention capacities, if available, are deployed right at the onset of the disease outbreak. In many cases this may not be possible. In this section, we investigate the impact of delaying the intervention time of testing and control on the disease progression within the population. Three intervention times are considered: at the onset of the pandemic outbreak (day 0 similar to the results in the previous section), delayed by one month and by two months (day 30 and day 60, respectively). Moreover, for the different intervention start dates, we solve for all intervention levels considered in the previous section (from T = 5,000 to T = 10,000 tests per day).

Fig. (7) compares the cumulative number of infections as a result of different testing and control intervention levels and dates. For each intervention level and intervention date, the results are broken down for each region besides providing the total values of all regions. As expected, the results confirm that delaying the intervention times, for the same intervention level, results in a higher number of infections per region and in total. Interestingly, for the highest intervention levels (T = 50,000 and T = 100,000 tests per day) delaying the intervention time results in significantly worse results compared to when intervention is performed earlier. Furthermore, the results confirm that in some cases delaying the intervention time would lead to an overall worse outcome than significantly reducing the intervention level but performing it

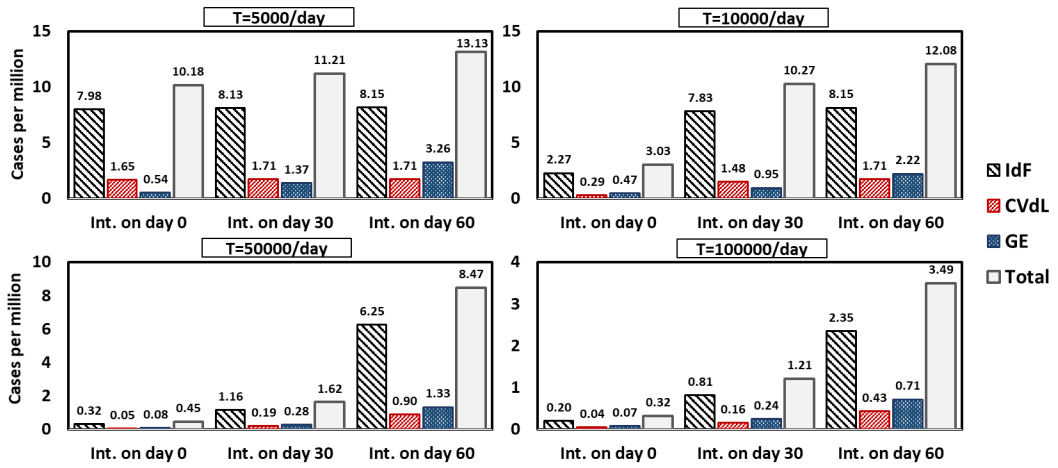

Figure 7: Comparison between the cumulative number of infections for each region as a result of different intervention start dates (on day 0, day 30 and on day 60) and for each intervention level.

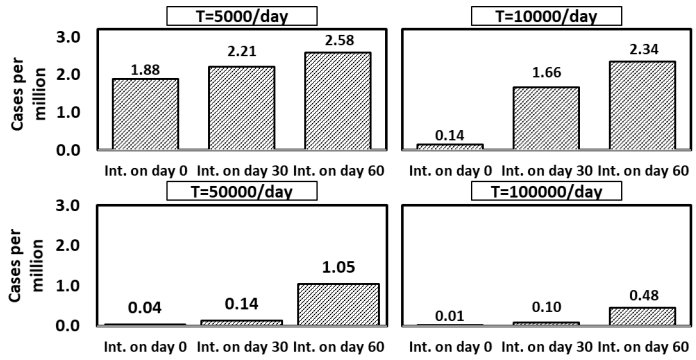

Figure 8: Comparison between the cumulative number of deaths (total of all regions) as a result of different intervention start dates (on day 0, day 30 and on day 60) and for each intervention level.

as early as possible. This is clear in the comparison between the results of T = 50,000 and T = 100,000 for an intervention on day 60 (total of 8.47 million and 3.49 million cases of infection, respectively), compared to the outcome of T = 10,000 tests per day for an intervention on day 0 (total of 3.03 million cases of infection). Moreover, this analysis holds for the resulting number of deaths, as is illustrated in Fig. (8), and highlight the usefulness of the proposed model in evaluating the trade-off between intervention level and time for effective preparedness strategies.

Finally, we investigate how the optimal allocation strategy of testing and control resources change as a function of the intervention time. Fig. (9) illustrates the percentage of testing capacity allocated for each region when different intervention dates are considered and for all intervention levels. As seen in the Figure, for all intervention levels, as the intervention time is delayed, the results suggest that it would be optimal to increase the resources allocated to the GE region and reduce it for the other regions. For example, for the low resources scenario (T = 5,000/day), the optimal allocation for early intervention (at day 0) is 30% for IdF, 14 % for CVdL and 56% for GE, whereas the optimal allocation for a delayed intervention (day 60) is 100% for the GE region and none for the others. The trend holds for all intervention levels; however, as more testing capacities are available, the proportion available for the other regions remains considerable.

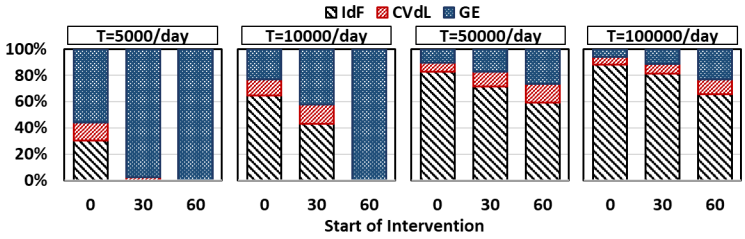

Figure 9: Comparison between the optimal allocation decisions of testing resources among regions (in percentage) as a function of different intervention start dates (on day 0, day 30 and on day 60) and for each intervention level.

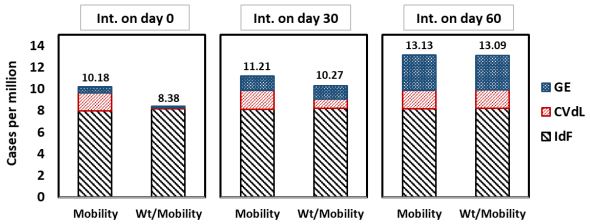

Figure 10: Comparison between the cumulative number of cases (total of all regions) as a result of different intervention start dates (on day 0, day 30 and on day 60). The case of intervention level = 5,000 tests/day.

6.3. Impact of prohibiting mobility between regions on optimal resource allocation and disease progression

In this section, we investigate the impact of prohibiting mobility between regions on the spread of the disease. Computational experiments indicate that, indeed, prohibiting mobility between regions might be another way to limit the spread of the disease, in particular at the early stages of the intervention. For clarity, we consider a single intervention level (T = 5,000 tests per day) and compare the results for the 3 intervention dates previously considered. Fig (10) compares the cumulative number of infections at each region, and their total for the scenario with mobility (Mobility) and with mobility prohibition (Wt/Mobility).

The results suggest that combining both early intervention (day 0) and mobility restriction leads to a significant reduction in the number of cases by around 1.8 million cases as seen in Fig. (10). The impact of mobility restriction is disproportional among the different regions, with regions which have a lower overall net mobility (CVdL and GE) benefiting more from this measure as opposed to the region with the highest net mobility (IdF), for which the mobility restriction actually leads to an increase in the local infections. Less significant impact for restricting mobility is observed as the testing and control intervention dates are delayed. This is clear for the insignificant impact on the number of cases when intervention is delayed by 2 months (intervention on day 60), even if mobility is restricted between regions.

Furthermore, we can evaluate the impact of restricting mobility on the disease progression in terms of the daily number of infections at each region. Fig. (11) confirms that for the earliest intervention date (day 0), restricting mobility results in an *earlier* rise in the number of infections for the IdF region, but with no significant change for the peak infection level. For CVdL and GE, the daily number of infections reduces considerably (flattening the curve), as seen in the Figure. As intervention dates are delayed, the infection curves maintain their characteristics in terms of peak levels and shape, regardless of whether or not mobility between regions is restricted. This means that less flattening of the curves occur in these cases.

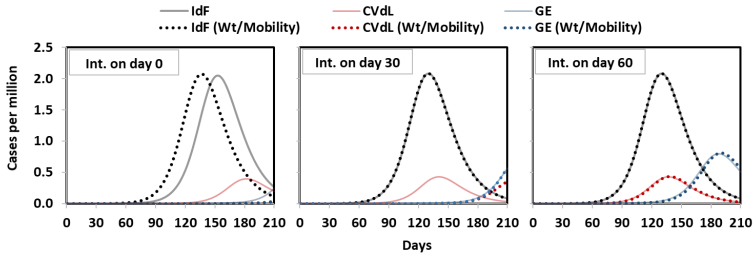

Figure 11: Comparison between the evolution of the daily number of infections with and without regional mobility, for each region and for every intervention start date. The case of intervention level = 5,000 tests/day).

6.4. Impact of equity on the testing resources allocation and disease progression among regions

Thus far, the results shown and analyzed do not consider equity in resource allocation, i.e., they seek to minimize the total new infections and untreated deaths in all regions, without accounting for the differences in the vulnerability levels of the regions. As mentioned earlier, an equity-driven objective considers these differences. The results in this section compare the non equity-driven results (for ease of discussion we call them the "standard" results) to the equity-driven results obtained by solving the MINLP model proposed with the equity objective function (29).

Fig (12) compares the standard objective results to the equity-based results, in terms of the objective function value (Fig. 12a) and in terms of testing capacity allocated for each region (Fig. 12b), for the different intervention levels. As seen in the Figures, the following observations arise:

i) For the objective function, the equity-driven solution ($\mathcal{O}_{EQUITY}$), indeed, has a reduced absolute difference in the objective values across the regions and for all cases, as seen in Fig. (12a). This is noted in the increase of the equity objective value (number of cases + number of untreated deaths) for the lowest impacted regions (CVdL and GE), compared to the standard solution ($\mathcal{O}$), and a respective decrease of the objective value for the highly impacted region (IdF). However, notice that, although the vulnerability levels of all regions are equivalent for all cases considered, the equity-driven solution does not have the same proportional impact on changing the objective function values for all the intervention levels. Indeed, the difference between the $\mathcal{O}$ and $\mathcal{O}_{EQUITY}$ results is more pronounced for the lowest intervention levels (T = 5,000/days and T = 10,000/days) compared to the higher intervention levels (T = 50,000/day and T = 100,000/day) in which cases the solutions are almost identical. This is because, by taking into account the vulnerability factor, the equity-driven solution seeks to minimize the *absolute* difference between regions, which is much higher for the former cases (e.g. the difference in the O value between IdF and GE is around 7.6 million cases for T = 5000/day) than for the latter ones (e.g. this difference is equal to just 130 *thousand* cases for T = 100,000 per day).

ii) To understand how the equitable solution is achieved by the optimal decisions, Fig. (12b) summarizes the allocation decisions of testing capacities for each region. The results show that, in order to achieve the equitable objective, the allocation of the testing capacities TC_{EQUITY} shift from the lower impacted regions (CVdL and GE) to the higher impacted region (IdF) compared to the standard solution TC. With lower testing capacity, the proportion of tests allocated for the IdF region is

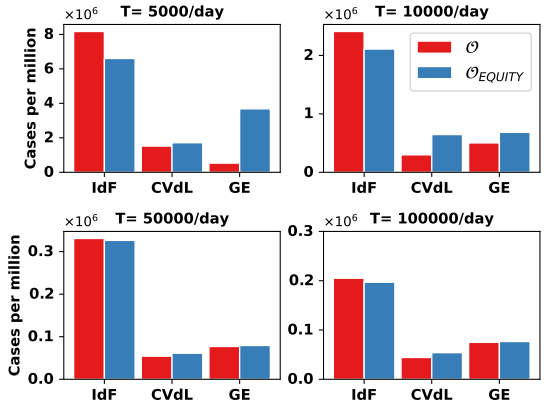

(a) Comparison between the objective function values (cumulative number of infections + deaths without hospitalization).

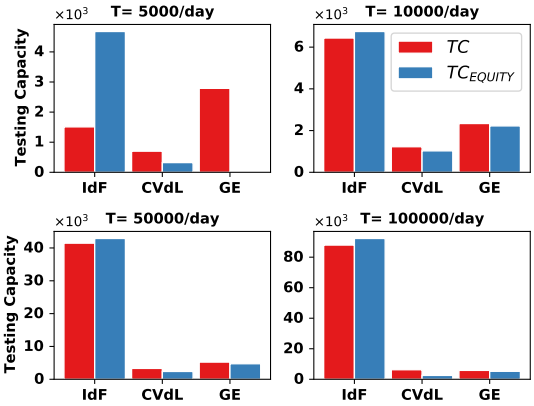

(b) Comparison between the optimal allocation of testing resources among regions.

Figure 12: Comparison between the standard vs the equity-driven solutions for each intervention level.

higher than in cases where testing capacities are high, as previously explained. Furthermore, the effect of the equity-driven solution on the number of cases hospitalized and deceased follows the same trend as that observed for the objective value. These results are illustrated in Appendix C.

Finally, the policymaker may evaluate the *inequity* level resulting from each allocation strategy by calculating the GINI score presented in Eq. (2c). Fig. (13) compares the inequity levels obtained by solving the allocation problem with the standard objective compared to the equity-driven objective. First, notice how, even for the standard solution, the inequity decreases as more resources are available. The inequity level starts at a level of 0.41 for the case of T = 5,000/day (1 being absolute inequity and 0 being absolute equity) and reduces constantly to an inequity level of 0.31 for the case of T = 100,000/day. Moreover, as expected, for all cases, the inequity level is lower for the solutions explicitly driven by the equitable objective, and remaining around a level of 0.27. Finally, notice that an inequity level remains in these solutions, since they still consider the effectiveness of reducing the global numbers of new infections and untreated deaths as a relevant objective, even if it maintains some level of inequity.

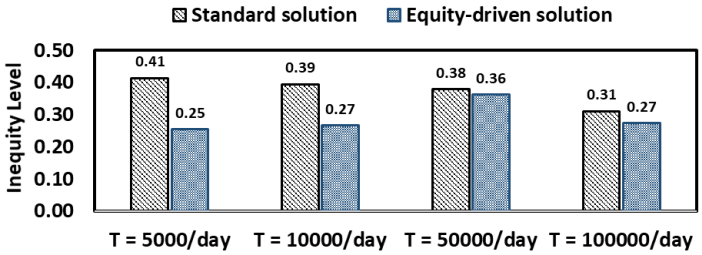

Figure 13: Comparison between the inequity level (GINI index score) between the standard solution and the equity-driven solution for the different intervention levels.

7. Conclusions

This paper presented a novel mixed-integer non-linear programming (MINLP) epidemic compartmental model for allocating limited testing and control resources to control the spread of an infectious disease. Our MINLP framework contributes to the current epidemiological operational research literature by: (1) a novel formulation for testing and control allocation decisions for both symptomatic and asymptomatic individuals in the population, and taking into account the positivity-rate of testing, (2) extending the pandemic compartmental model to consider different levels of infections severity and asymptomatic transmission of the disease, (3) a method to evaluate the vulnerability levels of the different impacted communities and a re-formulation of the objective function to consider equity in the allocation of testing and control resources based on the GINI index, (4) validating the possibility to solve the model for a wide variety of scenarios with explicit consideration of the non-linearity and showing the superiority of the results obtained by validation against real data.

We illustrate the usefulness of the proposed modeling framework for informing policymakers about the optimal allocation of limited testing and control capacities, and their impact on the pandemic progression. In particular, we consider a case study for the COVID-19 pandemic outbreak in France and explore a wide range of possible intervention times and levels.

Future research could address some of the limitations of this work, in particular with respect to the treatment of the inherent uncertainties in the disease transition parameters of the model, such as the rates of hospitalizations, recovery, severity of the disease or deaths, and their impact on the allocation decisions. Another interesting extension may consider the ability of the recovered population to become once again susceptible to the disease, which has been shown to be a possibility with the COVID-19 pandemic. Note that further extensions of the model may require the development of tailored solution algorithms, in particular if non-linearity is to be properly considered. Finally, such kind of modeling framework should be adopted by policymakers to inform decisions on actions and precautions for resilience to future pandemic outbreaks.

References

Alberti, P. M., Lantz, P. M., and Wilkins, C. H. (2020). Equitable pandemic preparedness and rapid response: lessons from covid-19 for pandemic health equity. *Journal of health politics, policy and law*, 45(6):921–935.

Aleta, A., Martin-Corral, D., y Piontti, A. P., Ajelli, M., Litvinova, M., Chinazzi, M., Dean, N. E., Halloran, M. E., Longini Jr, I. M., Merler, S., et al. (2020). Modelling the impact of testing, contact tracing and household quarantine on second waves of covid-19. *Nature Human Behaviour*, 4(9):964–971.

Braithwaite, I., Callender, T., Bullock, M., and Aldridge, R. W. (2020). Automated and partly automated contact tracing: a systematic review to inform the control of covid-19. *The Lancet Digital Health*.

Braveman, P. (2006). Health disparities and health equity: concepts and measurement. *Annu. Rev. Public Health*, 27:167–194.

Buhat, C. A. H., Duero, J. C. C., Felix, E. F. O., Rabajante, J. F., and Mamplata, J. B. (2020). Optimal allocation of covid-19 test kits among accredited testing centers in the philippines. *Journal of healthcare informatics research*, pages 1–16.

Büyüktahtakın, İ. E., des Bordes, E., and Kıbış, E. Y. (2018). A new epidemics–logistics model: Insights into controlling the ebola virus disease in west africa. *European Journal of Operational Research*, 265(3):1046–1063.

Dasaklis, T. K., Pappis, C. P., and Rachaniotis, N. P. (2012). Epidemics control and logistics operations: A review. *International Journal of Production Economics*, 139(2):393–410.

Dimitrov, N. B. and Meyers, L. A. (2010). Mathematical approaches to infectious disease prediction and control. In *Risk and optimization in an uncertain world*, pages 1–25. INFORMS.

Dong, E., Du, H., and Gardner, L. (2020). An interactive web-based dashboard to track covid-19 in real time. *The Lancet infectious diseases*, 20(5):533–534.

Ministère des solidarités et de la santé (2020). Nombre de lits de réanimation, de soins intensifs et de soins continus en france, fin 2013 et 2018. data retrieved on 20/11/2020, `https://drees.solidarites-sante.gouv.fr/etudes-et-statistiques/publications/article/nombre-de-lits-de-reanimation-de-soins-intensifs-et-de-soins-continus-en-france`.

Santé publique France (2020a). Données hospitalières relatives à l'épidémie de covid-19. data retrieved on 20/11/2020, `https://www.data.gouv.fr/fr/datasets/donnees-hospitalieres-relatives-a-lepidemie-de-covid-19/`.

Santé publique France (2020b). Données relatives aux résultats des tests virologiques covid-19. data retrieved on 20/11/2020, `https://www.data.gouv.fr/fr/datasets/donnees-relatives-aux-resultats-des-tests-virologiques-covid-19/`.

Duffey, R. B. and Zio, E. (2020). Prediction of covid-19 infection, transmission and recovery rates: A new analysis and global societal comparisons. *Safety Science*, 129:104854.

ECDC (2020). Novel coronavirus: three cases reported in france. accessed on 20/11/2020, `https://www.ecdc.europa.eu/en/news-events/novel-coronavirus-three-cases-reported-france`.

Eisenhandler, O. and Tzur, M. (2018). The humanitarian pickup and distribution problem. *Operations Research*, 67(1):10–32.

Ferguson, N., Laydon, D., Nedjati-Gilani, G., Imai, N., Ainslie, K., Baguelin, M., Bhatia, S., Boonyasiri, A., Cucunubá, Z., Cuomo-Dannenburg, G., et al. (2020). Report 9: Impact of non-pharmaceutical interventions (npis) to reduce covid19 mortality and healthcare demand. *Imperial College London*, 10:77482.

Guan, L., Prieur, C., Zhang, L., Prieur, C., Georges, D., and Bellemain, P. (2020). Transport effect of covid-19 pandemic in france. *Annual reviews in control*.

He, S., Peng, Y., and Sun, K. (2020). Seir modeling of the covid-19 and its dynamics. *Nonlinear Dynamics*, 101(3):1667–1680.

Hogg, J. D. and Scott, J. A. (2011). *HSL_MA97: a bit-compatible multifrontal code for sparse symmetric systems*. Science and Technology Facilities Council.

Hsiang, S., Allen, D., Annan-Phan, S., Bell, K., Bolliger, I., Chong, T., Druckenmiller, H., Huang, L. Y., Hultgren, A., Krasovich, E., et al. (2020). The effect of large-scale anti-contagion policies on the covid-19 pandemic. *Nature*, 584(7820):262–267.

INSEE, I. n. d. l. s. e. d. e. e. (2019a). Logements, individus, activité, mobilités scolaires et professionnelles, migrations résidentielles en 2016. accessed on 20/11/2020, `https://www.insee.fr/fr/statistiques/4171517?sommaire=4171558`.

INSEE, I. n. d. l. s. e. d. e. e. (2019b). Logements, individus, activité, mobilités scolaires et professionnelles, migrations résidentielles en 2016. accessed on 20/11/2020, `https://www.insee.fr/fr/statistiques/4171531?sommaire=4171558`.

Iwata, K. and Miyakoshi, C. (2020). A simulation on potential secondary spread of novel coronavirus in an exported country using a stochastic epidemic seir model. *Journal of clinical medicine*, 9(4):944.

Jordan, R. E., Adab, P., and Cheng, K. (2020). Covid-19: risk factors for severe disease and death.

Kermack, W. O. and McKendrick, A. G. (1927). A contribution to the mathematical theory of epidemics. *Proceedings of the royal society of london. Series A, Containing papers of a mathematical and physical character*, 115(772):700–721.

Lauer, S. A., Grantz, K. H., Bi, Q., Jones, F. K., Zheng, Q., Meredith, H. R., Azman, A. S., Reich, N. G., and Lessler, J. (2020). The incubation period of coronavirus disease 2019 (covid-19) from publicly reported confirmed cases: estimation and application. *Annals of internal medicine*, 172(9):577–582.

Li, R., Pei, S., Chen, B., Song, Y., Zhang, T., Yang, W., and Shaman, J. (2020). Substantial undocumented infection facilitates the rapid dissemination of novel coronavirus (sars-cov-2). *Science*, 368(6490):489–493.

Linton, N. M., Kobayashi, T., Yang, Y., Hayashi, K., Akhmetzhanov, A. R., Jung, S.-m., Yuan, B., Kinoshita, R., and Nishiura, H. (2020). Incubation period and other epidemiological characteristics of 2019 novel coronavirus infections with right truncation: a statistical analysis of publicly available case data. *Journal of clinical medicine*, 9(2):538.

MacIntyre, C. R. (2020). Case isolation, contact tracing, and physical distancing are pillars of covid-19 pandemic control, not optional choices. *The Lancet Infectious Diseases*, 20(10):1105–1106.

Madubueze, C. E., Dachollom, S., and Onwubuya, I. O. (2020). Controlling the spread of covid-19: optimal control analysis. *Computational and Mathematical methods in Medicine*, 2020.

Meltzer, M. I., Atkins, C. Y., Santibanez, S., Knust, B., Petersen, B. W., Ervin, E. D., Nichol, S. T., Damon, I. K., and Washington, M. L. (2014). Estimating the future number of cases in the ebola epidemic–liberia and sierra leone, 2014–2015.

Moatti, J.-P. (2020). The french response to covid-19: intrinsic difficulties at the interface of science, public health, and policy. *Nature*, 579:319–20.

Moghadas, S. M., Fitzpatrick, M. C., Sah, P., Pandey, A., Shoukat, A., Singer, B. H., and Galvani, A. P. (2020). The implications of silent transmission for the control of covid-19 outbreaks. *Proceedings of the National Academy of Sciences*, 117(30):17513–17515.

Mwalili, S., Kimathi, M., Ojiambo, V., Gathungu, D., and Mbogo, R. (2020). Seir model for covid-19 dynamics incorporating the environment and social distancing. *BMC Research Notes*, 13(1):1–5.

Omondi, E., Mbogo, R., and Luboobi, L. (2018). Mathematical modelling of the impact of testing, treatment and control of hiv transmission in kenya. *Cogent Mathematics & Statistics*, 5(1):1475590.

Öztoprak, F. and Javed, A. (2020). Case fatality rate estimation of covid-19 for european countries: Turkey's current scenario amidst a global pandemic; comparison of outbreaks with european countries. *world*, 21:24.

Pan, A., Liu, L., Wang, C., Guo, H., Hao, X., Wang, Q., Huang, J., He, N., Yu, H., Lin, X., et al. (2020). Association of public health interventions with the epidemiology of the covid-19 outbreak in wuhan, china. *Jama*, 323(19):1915–1923.

Park, Y. J., Choe, Y. J., Park, O., Park, S. Y., Kim, Y.-M., Kim, J., Kweon, S., Woo, Y., Gwack, J., Kim, S. S., et al. (2020). Contact tracing during coronavirus disease outbreak, south korea, 2020. *Emerging infectious diseases*, 26(10):2465–2468.

Rachaniotis, N. P., Dasaklis, T. K., and Pappis, C. P. (2012). A deterministic resource scheduling model in epidemic control: A case study. *European Journal of Operational Research*, 216(1):225–231.

Rajaonah, B. and Zio, E. (2020). Risk perception biases and the resilience of ethics for complying to covid-19-pandemic-related safety measures. *hal-03048334*.

Russell, T., Hellewell, J., Jarvis, C., Van-Zandvoort, K., Abbott, S., Ratnayake, R., Flasche, S., Eggo, R., Kucharski, A., nCov working group, C., et al. (2020). Estimating the infection and case fatality ratio for covid-19 using age-adjusted data from the outbreak on the diamond princess cruise ship. medrxiv. 2020 mar 5. *DOI*, 10(2020.03):05–20031773.

Sun, L., DePuy, G. W., and Evans, G. W. (2014). Multi-objective optimization models for patient allocation during a pandemic influenza outbreak. *Computers & Operations Research*, 51:350–359.

Sung, H., Yoo, C.-K., Han, M.-G., Lee, S.-W., Lee, H., Chun, S., Lee, W. G., and Min, W.-K. (2020). Preparedness and rapid implementation of external quality assessment helped quickly increase covid-19 testing capacity in the republic of korea. *Clinical chemistry*, 66(7):979–981.

van den Driessche, P. (2008). *Deterministic Compartmental Models: Extensions of Basic Models*, pages 147–157. Springer Berlin Heidelberg, Berlin, Heidelberg.

Wächter, A. and Biegler, L. T. (2006). On the implementation of an interior-point filter line-search algorithm for large-scale nonlinear programming. *Mathematical programming*, 106(1):25–57.

Wassie, G. T., Azene, A. G., Bantie, G. M., Dessie, G., and Aragaw, A. M. (2020). Incubation period of sars-cov-2: a systematic review and meta-analysis. *Current Therapeutic Research*, page 100607.

Wells, C. R., Townsend, J. P., Pandey, A., Moghadas, S. M., Krieger, G., Singer, B., McDonald, R. H., Fitzpatrick, M. C., and Galvani, A. P. (2020). Optimal covid-19 quarantine and testing strategies. *Nature Communications*, 12(1):1–9.

WHO, W. H. O. et al. (2020). Covid-19 weekly epidemiological update, 29 december 2020.

Wölfel, R., Corman, V. M., Guggemos, W., Seilmaier, M., Zange, S., Müller, M. A., Niemeyer, D., Jones, T. C., Vollmar, P., Rothe, C., et al. (2020). Virological assessment of hospitalized patients with covid-2019. *Nature*, 581(7809):465–469.

Wu, Z. and McGoogan, J. M. (2020). Characteristics of and important lessons from the coronavirus disease 2019 (covid-19) outbreak in china: summary of a report of 72 314 cases from the chinese center for disease control and prevention. *Jama*, 323(13):1239–1242.

Yan, B., Zhang, X., Wu, L., Zhu, H., and Chen, B. (2020). Why do countries respond differently to covid-19? a comparative study of sweden, china, france, and japan. *The American Review of Public Administration*, 50(6-7):762–769.

Yarmand, H., Ivy, J. S., Denton, B., and Lloyd, A. L. (2014). Optimal two-phase vaccine allocation to geographically different regions under uncertainty. *European Journal of Operational Research*, 233(1):208–219.

Zhou, F., Yu, T., Du, R., Fan, G., Liu, Y., Liu, Z., Xiang, J., Wang, Y., Song, B., Gu, X., et al. (2020). Clinical course and risk factors for mortality of adult inpatients with covid-19 in wuhan, china: a retrospective cohort study. *The lancet*.